Modeling active muscle behavior for emergency braking simulations

M. Behr[b,*], P.J. Arnoux[b], T. Serre[b], K. Kayvantash[a], C. Brunet[b]

[a]*MECALOG sarl, BU Safety and Biomechanics, Bld Pierre Dramard, 13916 Marseille Cedex 20, France*
[b]*Laboratoire de Biomécanique Appliquée, INRETS/UnivMed, Bld Pierre Dramard 13016 Marseille, France*

Abstract

Numerical and physical models used in car crash simulations hardly take into account the active behavior of car occupants, in terms of positions and muscular contractions. However, muscles seem to have a significant influence on kinematics and energy dissipation at least up to a reasonable acceleration level. We present in this paper a finite element musculoskeletal model developed for the RADIOSS crash code [14], focusing on lower limbs, which offers the possibility to reproduce muscular activity of car occupants in crash situations. Skeletal muscle mechanical behavior is based on a phenomenological approach, and depends on a reduced number of input parameters. In terms of geometry, muscles are represented with visco-elastic solids that are controlled in the direction of fibers by a set of 1D contractile springs. Validation has been achieved by the observation of movements resulting from particular contraction configurations and by comparing simulations and previously performed experiments on volunteers.

Keywords: Biomechanics; Muscles; Simulation; Emergency braking; Crashworthiness; Injury mechanism

1. Introduction

One particular feature of a car driver in a real crash situation is its capacity to anticipate the impact, by changing its position in the seat and by suddenly and strongly acting on the brake pedal [1,2].

This global muscular behavior prior to impact is not taken into account in most recent human models dedicated to car crash simulations, although muscle tone seems to have a significant influence on the global kinematics (at least up to a reasonable level of acceleration) [3,4,5]. It seems also that bracing of skeletal muscles participate to the fracture of the bones they surround, by enhancing force transmission and reducing energy absorption [6,7].

The main objective of our study is to develop a finite element model that can help in understanding the contribution of muscle bracing under impact, and therefore enhance the evaluation of security systems on commercial cars, by taking into account this fundamental property of muscles, i.e. to modify their mechanical properties when activated. We present in this paper the different stages of development of this model, focusing on the lower limb. Validation was achieved by comparing our simulation results to previously performed experiments on volunteers.

2. Methods

More than 500 CT scan images were taken from a volunteer male close to the 50th percentile, focusing on the lower limb. A software platform was developed for the semi automated analysis of these images [8], i.e. the contouring of all identified anatomic items. In the particular case of muscles detection and contouring, the analysis was fully manual and performed by experienced anatomists in order to separate as much as possible all muscular heads. As tendinous parts were difficult to identify (because of the poor contrast of frontiers and sometimes extremely low thickness of fascias), tendons geometry was extrapolated from muscles bodies extremities to their theoretical insertions on bones. This geometry acquisition process lead to the definition of approximately 20 independent muscle bundles (Fig. 1). These musculo-tendinous geometries were implemented on the MECALOG/LBA LLMS skeletal model (Lower

* Corresponding author. Tel.: +33 4 91 51 91 26; E-mail: behr@cats.rwth-aachen.de

Computational Fluid and Solid Mechanics 2005
K.J. Bathe (Editor)

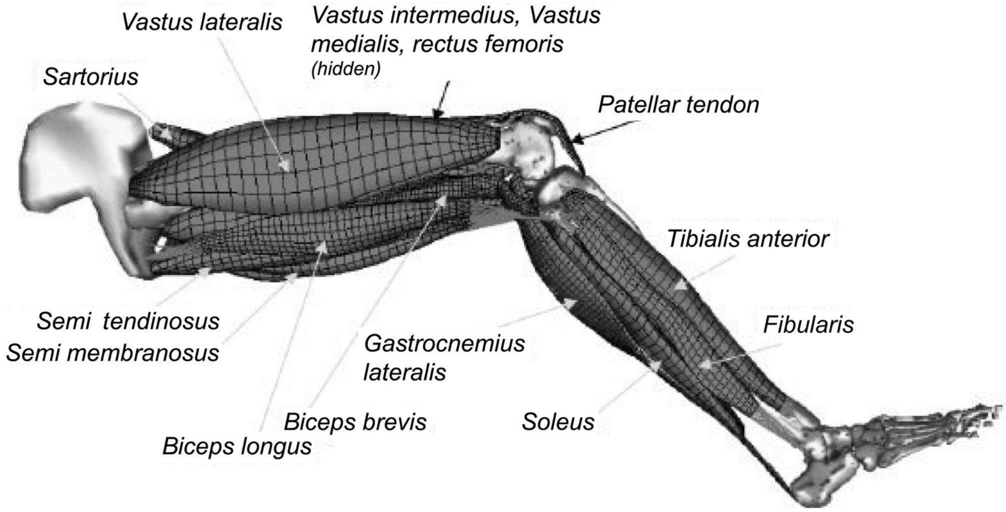

Fig. 1. Lower limb mesh.

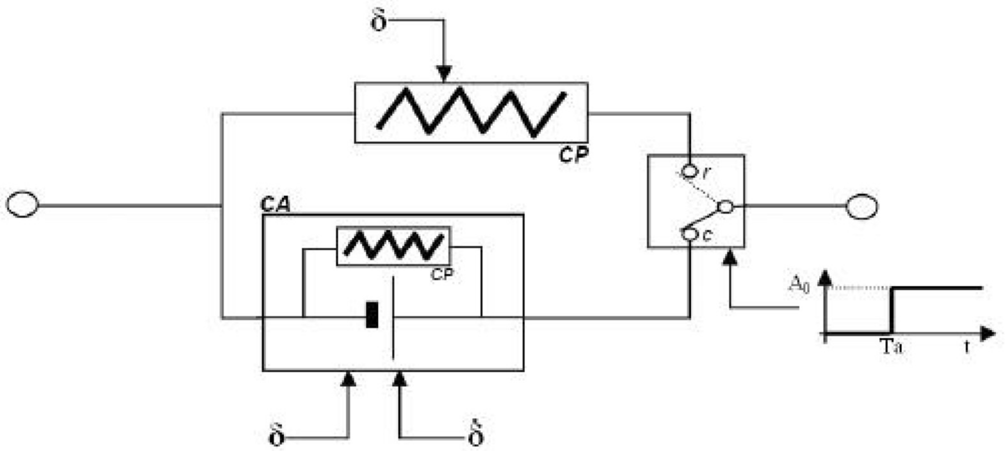

Fig. 2. Schematic illustration of the contraction unit. δ is the instantaneous length of the muscle, A_0 the level of activation and T_a the instant of activation.

Limb Model for Safety [9]), as both geometry acquisitions were performed on the same set of images.

As a first approach, each muscle is considered as the sum of a tendon part, a passive incompressible mass acting as an energy absorber, and a set of action lines (muscle fibers) integrating the possibility to actively shorten in order to simulate muscle contraction.

Tendons are modeled by a bundle of springs running from one same origin node on the bone to each node of the 3D mesh extremity. These springs have a linear elastic behavior in traction, with an elastic modulus of 150 MPa.

Visco-elastic orthotropic quasi-incompressible bricks play the role of dampers and inertial components. This hexahedral mesh is based on the geometry of the external surfaces extracted from the CT scan analysis. The elastic modulus was set to 5.32 MPa in both directions orthogonal to the fibers. In the direction of the fibers, the elastic modulus was set to 1 MPa, as mechanical properties result from the effect of 1D fiber elements described hereafter.

Muscle fibers are composed of series of 1D rheologic elements – contraction units (CU) – running from one proximal to its corresponding distal tendon spring end, and merged to the nodes of the muscle bricks.

These CUs play the role of macroscopic sarcomas, and are composed of two mechanical parts: a non linear elastic element (CP) and an active element (CA) (Fig. 2).

Their mechanical formulation derives from Zajac's musculotendon model [10] and are given by Eqs. (1) and (2) for the ith CU:

$$F_i^{CP}(\delta_i) = \frac{4F_{mo}}{L_{mo}^2}(n\delta_i + nL_{oi} - L_{mo})^2 \quad (1)$$

$$F_i^{CA}(\delta_i, t) = F_{mo}A(t)f_1(\delta_i)f_2(\dot{\delta}_i) \quad (2)$$

where F^{CP} and F^{CA} are the forces across elements CP and CA respectively, F_{mo} is the maximum force the considered muscle can exert at length L_{mo} (known in literature as the *optimal muscle length*), n is the number of contraction units along one fiber, L_{oi} and δ_i are the instantaneous length and the relative elongation/contraction of the contraction unit i respectively, (f_1) and f_2) are known in literature as the *Isometric Force-Length Relation* and the *Isotonic Force-Velocity Relation* respectively, and $A(t)$ is the percentage of activation function (0 when the muscle is not braced and 1 when the muscle is fully activated).

We can note from these equations that muscle activation stands on two fundamental parameters, the optimal length L_{mo} and the maximal isometric force F_{mo}, that have now to be determined.

Since the length of each muscle varies as a function of the actual position of the limb, its optimal length is considered here as the one corresponding to the joints configuration that would lead to the maximum torque. Based on the experimental joint torque curves reported by Hoy et al. [11], we defined four different 'optimal positions'. In each of these positions, we also identified muscles responsible for positive torque generation that should therefore be at their optimal length:

Pos.1: knee fully extended, 15° plantar flexed ankle: gastrocnemius and tibialis anterior muscles;

Pos.2: 10° dorsal flexed ankle: soleus muscles;

Pos.3: 50° flexed hip, 35° flexed knee: hamstrings muscles.

Pos.4: 50° flexed hip, 60° flexed knee: quadriceps, adductors, sartorius and slender muscles.

Table 1 summarizes optimal muscle lengths as measured with our model, along with the minimum and maximum lengths each muscle can have according to the limb position. Concerning F_{mo}, we chose the values reported by Delp [12], simply adding a correction factor depending on the true volumes of muscles measured on our model. Results are summarized in Table 1, column 5.

We ended up with a model composed of 146 different mechanical parts, with approximately 50,000 elements with a minimum initial time step of 0.4×10^{-3} ms.

Table 1
Musculo-tendinous actuators parameters (L_M and L_m are the maximum and minimum length of the muscle respectively, depending on the limb position)

Muscle	L_{mo} (mm)	L_M/L_{mo}	L_m/L_{mo}	F_{mo} (N)
Rectus femoris	375.0	1.18	0.90	616
Vastus Lateralis	395.6	1.06	0.92	2241
Vastus Medialis	387.9	1.05	0.92	1130
Biceps (short head)	355.6	1.05	0.86	97
Biceps (long head)	486.6	1.14	0.72	436
Semimembranosus	451.5	1.13	0.83	568
Semitendinosis	472.6	1.19	0.76	140
Sartorius	461.8	1.18	0.84	85
Gracilis	433.3	1.20	0.84	71
Gastrocnemius L	488.0	1.07	0.91	2112
Gastrocnemius M	476.0	1.07	0.93	2112
Soleus	425.8	1.03	0.92	3331
Tibialis anterior	438.5	1.03	0.94	611

3. Model validation

The global behavior of isolated bundles, i.e. the force measured at each muscle insertions and resulting either from their passive or active behavior, was first checked. Simulation and theoretical curves appeared very concordant, and this was true both for braced and relaxed states, and both for traction or compression situations.

In a second step, we also checked the contribution of muscles in physiological movements. Different groups of muscles were successively braced and relaxed, as the result in terms of induced bones relative movements were recorded. These simulations showed the ability of the model to perform any wanted movement, simply by entering before the simulation the state curve (level of activation against time) of each muscle. After these two preliminary validation steps, we simulated the emergency braking situation, as it was defined by previous experiments on volunteers [13]. The conditions of the simulation are illustrated in Fig. 3. The Lower limb model was linked to a finite element model of the HYBRID III dummy. The ankle angle was set to 13° of plantar flexion, the knee angle to 55° of flexion, and the hip angle to 83° of flexion. Muscle activation was set to 55% for quadriceps muscles, to 25% for hamstrings muscles, to 43% for the triceps of the leg, and to 18% for the Tibialis anterior muscle (mean values of our experiments on volunteers).

After a delay of approximately 30 ms, the resulting force on the brake pedal reached a steady state of 75 daN, while volunteers exerted a mean force on the brake pedal of 80 daN.

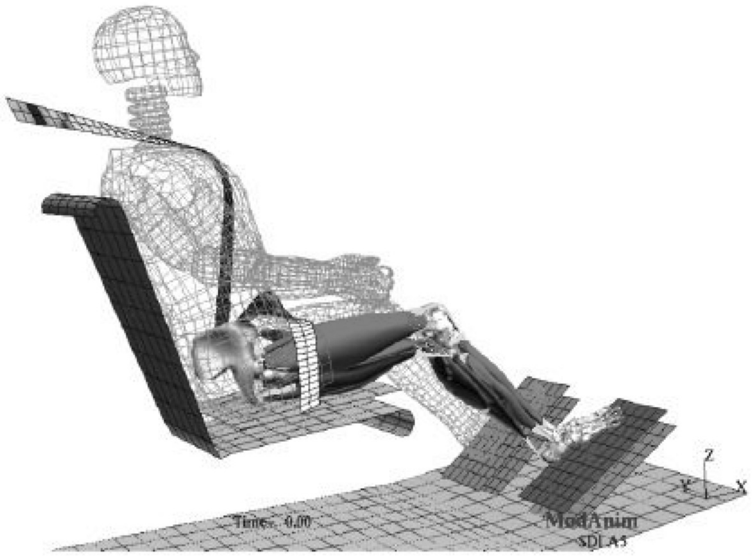

Fig. 3. Model validation: simulation of an emergency braking with braced muscles.

4. Conclusion

Contraction units, implemented within the muscle body, can suddenly shorten when activated, inducing a global shortening of the muscle. This shortening induces a force at the two insertion points, and modifies the mechanical properties of the muscle body (in terms of elastic modulus for example). Therefore, the finite element model presented here offers a suitable tool to investigate injuries mechanisms involved in car crash situations, taking into account the possible effect of muscle bracing.

The simulation of an emergency braking, in the very same configuration as the one resulting from experiments on volunteers, showed the ability of the model to reproduce the initial muscle pre-activation that should be applied to human models for frontal car crash studies.

Short term improvements should include a graduation of the activation (as the force generated by muscles is yet too sudden). Acceleration sensors could also be integrated within the muscle body. Over a preset threshold, these sensors would force the braced muscle to relax, as experienced in real life in the case of protective reflex muscular reactions.

References

[1] Manning P, Angus Wallace W, Roberts AK, Owen CJ, Lowne RW. The position and movement of the foot in emergency manœuvres and in the influence of tension in the achilles tendon. SAE paper no. 973329, 1997.

[2] Owen C, Roberts P, Lowne R. Positioning and bracing of the lower leg during emergency braking – a volunteer study. In: Proc of the IRCOBI Conference, Göteborg, Sweden 1998, pp. 147–159.

[3] Armstrong RW, Waters HP, Stapp JP. Impact tests show restraining force of legs might be used to reduce crash effects. SAE J 1970;78(2):32–37.

[4] Hendler E, O'Rourke J, Schulman M, Katzeff M, Domzalski L, Rodgers S. Effects of head and body position and muscular tensing on response to impact. SAE paper no. 741184, 1974.

[5] Begeman PC, King AI, Levine RS, Viano DC. Biodynamic response of the musculoskeletal system to impact acceleration. SAE paper no. 801312, 1980.

[6] Klopp G, Crandall J, Hall G, Pilkey W, Hurwitz S, Kuppa S. Mechanisms of injury and injury criteria for the human foot and ankle in dynamic axial impacts to the foot. In: Proc of the IRCOBI Conference, Brunnen, Switzerland, 1997, pp. 171–182.

[7] Kitagawa Y, Ichikawa H, King AI, Levine RS. A severe ankle and foot injury in frontal crashes an dits mechanism. SAE paper no. 983745, 1998.

[8] Bidal S, Serre T, Kayvantash K, Fieschi M, Bonnoit J. Semiautomatic 3D reconstruction and meshing of organs from 2D contours. In: Proc of the 7th Congrès Numérisation 3D – Human Modelling, Paris, France 2002, pp. 7–13.

[9] Arnoux P-J, Thollon L, Behr M, Kayvantash K, Cavallero C, Brunet C. Advanced lower limb finite element model for human tolerance evaluation. In: Proc of the IXth International Symposium on Computer Simulation in Biomechanics, Sydney, Australia 2003, p. 13.

[10] Zajac FE. Muscle and tendon: properties, models, scaling

and application to biomechanics and motor control. CRC Crit Rev Biomed Eng 1989;17:359–411.

[11] Hoy G, Zajac FE, Gordon ME. A musculoskeletal model of the human lower extremity: the effect of muscle, tendon, and moment arm on the moment-angle relationship of musculotendon actuators at the hip, knee and ankle. J Biomech 1990;23(2):157–169.

[12] Delp S. Parameters for a model of the lower limb, http://www.isbweb.org/data/delp/

[13] Behr M, Thiery C, Poumarat G, Serre T, Arnoux PJ, Brunet C. Muscular activation during emergency braking: an experimental approach. Arch Physiol Biochem 2003;111:13.

[14] RADIOSS users' manual, version 44, 2004.